Quantum dot emitters in two-dimensional photonic crystals of macroporous silicon

Stefan Richter, Martin Steinhart, Herbert Hofmeister, Margit Zacharias, and Ulrich Gösele
Max-Planck-Institute of Microstructure Physics, Weinberg 2, D-06120 Halle, Germany

Nikolai Gaponik and Alexander Eychmüller
Institute of Physical Chemistry, University of Hamburg, Grindelallee 117, D-20146 Hamburg, Germany

Andrey L. Rogach
Department of Physics and Center for Nanoscience (CeNS), Ludwig-Maximilians-University Munich, Amalienstrasse 54, D-80799 München, Germany

Joachim H. Wendorff
Institut für Physikalische-, Kern- und Makromolekulare Chemie, Philipps University Marburg, Hans-Meerwein-Strasse, 35032 Marburg/Lahn, Germany

Stefan L. Schweizer, Andreas von Rhein, and Ralf B. Wehrspohn[a)]
Department of Physics, University of Paderborn, Warburgerstrasse 100, D-33098 Paderborn, Germany

(Received 29 September 2004; accepted 11 August 2005; published online 30 September 2005)

We report on the incorporation of semiconductor quantum dots as internal emitters into two-dimensional photonic crystals of macroporous silicon. For this purpose we prepared composite nanotubes within the pores consisting of quantum dots embedded in a polymeric matrix. A spectral modification of the emission by the surrounding photonic crystal is demonstrated for mercury telluride quantum dots when the emission coincides with the photonic band gap of the Si photonic crystal. © *2005 American Institute of Physics*. [DOI: 10.1063/1.2081123]

Photonic band-gap materials have been studied extensively in recent years. In particular, the modification or even the inhibition of light emission from internal sources has attracted considerable interest. Approaches based on specifically designed epitaxially grown quantum well systems are widely used to realize internal emitters in two-dimensional (2D) photonic crystals.[1] In three dimensions photonic crystal structures have been infiltrated with laser dyes or colloidal quantum dot (QD) suspensions.[2–4] Here we report on the controlled incorporation of colloidal semiconductor QDs (Refs. 5–8) into 2D photonic crystals consisting of macroporous Si (Ref. 9) by preparing QD/polymer composite microtubes within their pores.

The integration of internal emitters into Si-based photonic crystals was realized with implantation methods[10] or self-assembled QDs.[11] The incorporation of internal emitters in electrochemically etched macroporous silicon has not been demonstrated yet. Furthermore, a spectral overlap of their emission and photonic band structure (preferably a photonic band gap) is necessary. This can be accomplished by the proper choice of the emitter and a respective adjustment of the lattice constant of the photonic crystal. The lattice constants of macroporous Si can be adjusted via lithography to any value between $a=500$ nm and a few microns. For a lattice constant of $a=700$ nm the fundamental band gap (TE polarization) is around 1500 nm. Colloidal HgTe QDs with diameters ranging from 3 to 6 nm represent an emitting system that has an emission wavelength coinciding with this spectral range.[12] Quantum confinement increases their electronic band gap, which amounts to −0.15 eV for bulk HgTe, to the average value of 0.83 eV. The size distribution of the particles causes a broadening of the luminescence spectrum from 1300 to 1700 nm, which is of use to study the emission modification under the influence of the photonic band gap. The lifetime of the luminescence is about 10 ns, nearly exponential and varies with the concentration of nanocrystals.[13]

To incorporate the QDs into the macroporous Si we prepared QD/polymer composite tubes within the pores. By the wetting method[14] HgTe QDs were synthesized in water as previously reported[12] and were transferred to toluene by a stabilizer exchange.[15] The suspensions were mixed with 1 wt % solutions of poly(methyl methacrylate) (PMMA, Mw=120 000 g/mol) and polystyrene (PS, Mw=250 000 g/mol) in the same solvent. To wet the templates, the polymeric solutions containing the dispersed QDs were dropped on the macroporous Si at ambient conditions. After the evaporation of the toluene, the residual film of solidified polymer/QD composite material on the surface of the template was mechanically removed. To investigate whether it is actually possible to move the QDs into the tube walls, and if so, to what extent they form clusters within the polymeric matrix, we employed transmission electron microscopy (TEM). For this purpose we wetted ordered porous alumina[16] with a pore diameter of 55 nm and a pore depth of 50 μm with a mixture of HgTe QDs and PS at a weight ratio of 1:10 in toluene. We selected ordered porous alumina as a template, because it is easier to cut and because the higher proportion of the sample volume occupied by the tube walls facilitates the detection of the QDs. However, we assume that the use of macroporous silicon as a template yields a similar arrangement of QDs. We embedded the wetted templates in epoxy resin and prepared ultrathin slices with a thickness of a few tens of nanometers, as obvious from their interference colors.

The evaluation of the obtained micrographs revealed that small clusters of QDs with dimensions of the order of 10 nm

[a)]Electronic mail: wehrspohn@physik.uni-paderborn.de

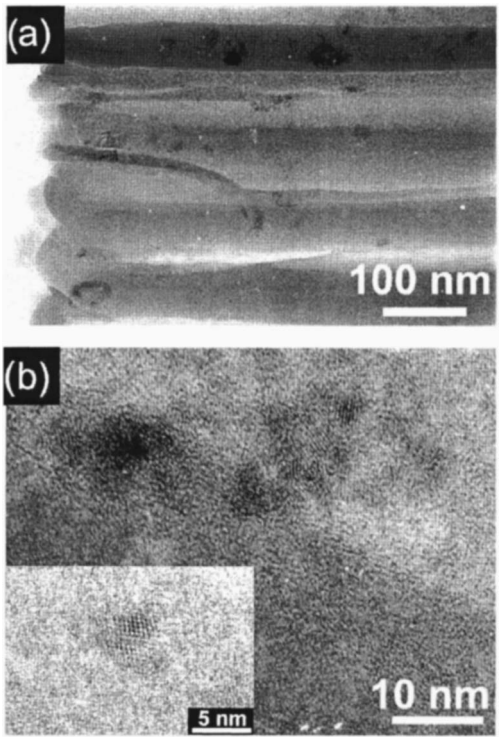

FIG. 1. Transmission electron micrographs of ultrathin sections of porous alumina (pore diameter: 55 nm; pore depth: 50 μm) wetted with a 1/10 mixture HgTe/PS. (a) Overview (on the left: bottoms of the template pores). (b) high-resolution image of a QD cluster within a tube wall (the dark strip from the top left to the bottom right is a pore wall consisting of alumina). Inset: individual QD within a tube wall.

had been formed. Figure 1(a) shows the hemispherical blind ends of the pores on the left. Within the pores, QD clusters appear as spots that are somewhat darker than their surrounding. Figure 1(b) represents a typical cluster consisting of a few QDs as observed at a higher magnification. It is located adjacent to an alumina pore wall, discernible as dark strip extending from top left to bottom right. In contrast to PS and the amorphous alumina wall, the QDs are crystalline and thus exhibit lattice fringes. Occasionally, individual QDs dispersed within the tube walls were also detected. An example is shown in the inset of Fig. 1(b). Since the QDs even occur in the vicinity of the blind ends of the template pores, they had been moved over a distance of several tens of microns in the course of the wetting procedure.

The QD/polymer tubes generally exhibit a strong photoluminescence (PL) signal corresponding to that of colloidal HgTe QDs suspended in toluene. This was studied for HgTe/PS composite tubes prepared by wetting ordered porous alumina (pore diameter: 350 nm) with solutions containing polymer/QDs at a weight ratio 10:1 [Fig. 2(a)]. Porous alumina was selected as a matrix here because it does not absorb or emit in the energy range where the QD emitters do emit. In addition, no coincidence with a photonic band gap is to be expected for the selected interpore distances.

We measured the PL spectra of hybrid systems consisting of the polymer/QD tubes well aligned within the porous alumina templates. Prior to the measurements, the residual material on the surface was carefully removed to uncover the pore openings and to make sure that the PL originates from QDs embedded within the tube walls. The maximum occurred at 0.85 eV, as it was the case of HgTe QDs in toluene solution.

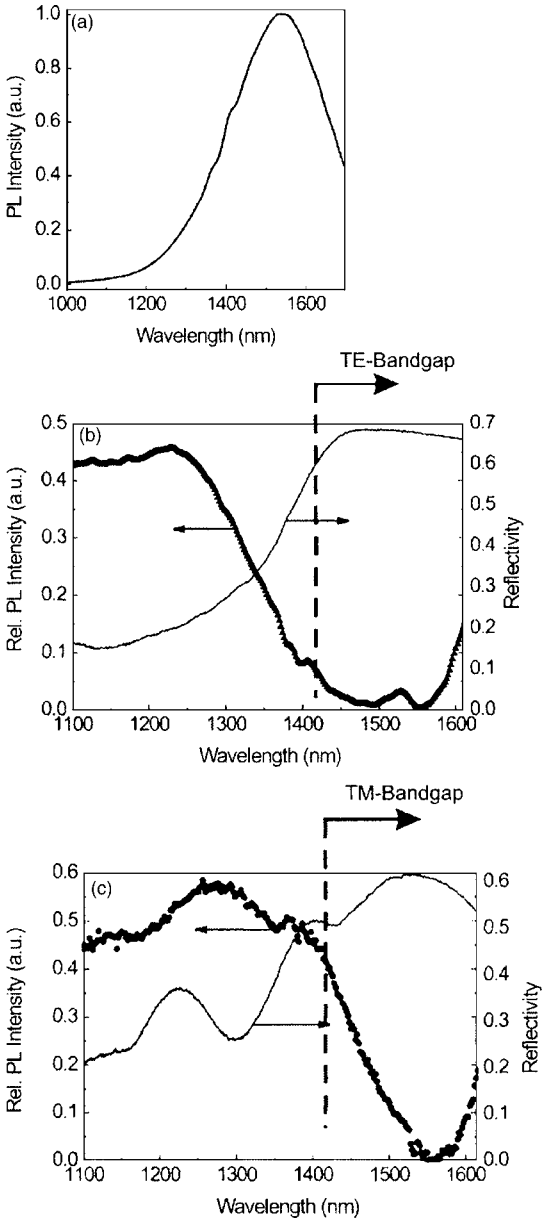

FIG. 2. Measurements: (a) free space PL spectrum of HgTe/PS tubes; (b) PL spectra of HgTe QDs in a hexagonal 2D photonic crystal of macroporous silicon (lattice constant 700 nm, TE polarization, $r/a=0.45$), normalized to the free space emission spectrum, compared to the corresponding reflection measurement; (c) same as (b) for TM polarization.

In order to investigate the modification of the emission spectrum of the QDs in a photonic crystal, a hexagonal 2D photonic crystal of macroporous silicon (lattice constant 700 nm, $r/a=0.45$) was prepared and infiltrated with HgTe/PS composite (weight ratio PS:HgTe of 10:1). The QDs were excited by an argon laser (488 nm) with incidence parallel to the pores axes. For better comparison with the 2D band structure, the emitted light was detected in the plane of periodicity of the 2D crystal for both TE and TM polarizations. The maximum acceptance angle of the off-axis parabolic mirror is about 24.6°.

The partial spectral overlap of the HgTe luminescence and the fundamental band gap allows only the investigation of the upper band edge. Comparing the photoluminescence (PL) spectra to reflection measurements, a coincidence of the decrease in PL intensity and the high reflectivity for wavelengths above 1300 nm (TE) and 1400 nm (TM), respec-

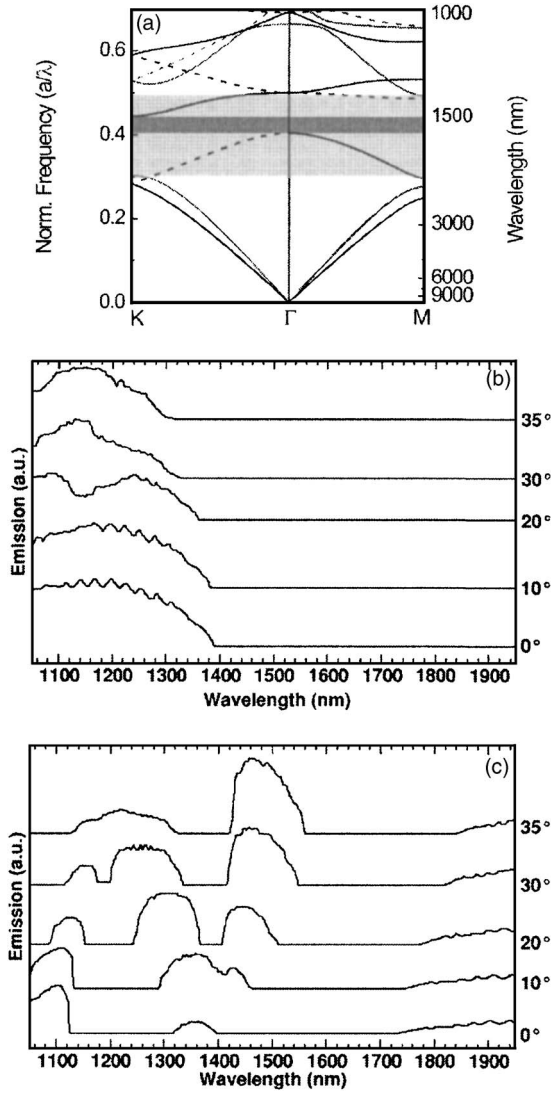

FIG. 3. Numerical calculation: (a) band structure of the 2D photonic crystal ($r/a=0.45$). Light gray corresponds to TE polarization and dark gray to TM polarization. The dashed lines are bands that cannot couple to plane waves due to symmetry reasons. (b), (c) Emission spectra of a source placed in the middle of a photonic crystals along ΓM (power flow normalized to power flow without photonic crystals). (b) TE-polarized emission spectra for different acceptance angles. Only a slight change of the band edge is observed changing the angle. (c) TM-polarized emission spectra for different acceptance angles. A strong dependence of the band edge is observed with the increasing angle.

tively, occurs, as shown in Figs. 2(b) and 2(c), respectively. The PL spectra are normalized to the free space emission of the HgTe/PS tubes. The photonic band gap prevents the existence and propagation of light in the crystal.

We calculated the band structure of the 2D photonic crystal [Fig. 3(a)] by using the MIT package.[17] The emission characteristics of the QD were computed by using a commercially available time-harmonic Maxwell-Solver (FEMLAB^{TM}). The source has been placed in the middle of a crystal build up from about 41 rows (ΓM) with air around it.

For both polarizations we expect from the band structure and the FEM-emission calculation that there is no emission for wavelengths larger than 1400 nm ($a/\lambda=0.5$) (Fig. 3). However, this effect is less pronounced for the TM band gap than for the TE band gap (Fig. 2). We therefore took into account the acceptance angle of detection optics being about 24.6°. For the TE polarization, there is very little change in the cut-off wavelength of the emission with increasing angle ranging from 1400 nm for direct incidence up to 1350 nm for an angle of 30°. For wavelengths smaller than 1400 nm, the second band of the TE mode in Γ-M direction allows coupling from plane waves and also from the emitter, resulting in an increase of the emission spectra and a decrease in reflectivity. For the TM polarization, there is a strong angular dependence of the emission. The cut-off wavelength increases with angle from 1400 nm for direct emission up to 1550 nm for an angle of 30°. This explains why photoluminescence is already observable at 1550 nm, far below the TM band gap in the Γ-M direction. Between 1300 and 1400 nm, there is a symmetric band that can couple to the plane waves and to the emitter. Thus, there is first an increase in QD emission and decrease of the reflectivity. However, for a wavelength around 1200 nm, there is again a stopgap. This can be seen in the increase of reflectivity around 1200 nm and a slight decrease in the QD emission [Fig. 2(c)]. Again, the decrease is significantly washed out because this stopgap vanishes for angles larger than 20° [Fig. 3(c)].

In conclusion, we presented a method to functionalize photonic crystals of macroporous silicon with QDs as internal emitters. The QDs are homogeneously incorporated in polymer tubes, forming replicas of the 2D photonic crystal. The spectral modification of the HgTe QD emission by the photonic crystal is demonstrated and in good agreement with numerical simulations. The advantage of our approach is the extensibility to other colloidal QDs and/or other photonic crystal structures.

The authors gratefully acknowledge financial support by DFG (Deutsche Forschungsgemeinschaft) under Za 191/13, RO 2345/1, WE 2637/6, STE1127/2, and WE 496/26.

[1] O. Painter, R. Lee, A. Yariv, A. Scherer, J. OBrien, P. Dapkus, and I. Kim, Science **284**, 1819 (1999).
[2] S. V. Gaponenko, V. N. Bogomolov, E. P. Petrov, A. M. Kapitonov, D. A. Yarotsky, I. I. Kalosha, A. A. Eychmueller, A. L. Rogach, J. McGilp, U. Woggon, and F. Gindele, J. Lightwave Technol. **17**, 2128 (1999).
[3] M. Megens, J. Wijnhoven, A. Lagengijk, and W. Vos, Phys. Rev. A **59**, 4727 (1999).
[4] P. Lodahl, A. F. van Driel, I. S. Nikolaev, A. Irman, K. Overgaag, D. Vanmaekelbergh, and W. L. Vos, Nature (London) **430**, 654 (2004).
[5] L. E. Brus, J. Chem. Phys. **80**, 4403 (1984).
[6] H. Weller, Angew. Chem., Int. Ed. Engl. **32**, 41 (1993).
[7] C. B. Murray, D. J. Norris, and M. G. Bawendi, J. Am. Chem. Soc. **115**, 8706 (1993).
[8] A. P. Alivisatos, Science **271**, 933 (1996).
[9] A. Birner, R. B. Wehrspohn, U. Gösele, and K. Busch, Adv. Mater. (Weinheim, Ger.) **13**, 377 (2001).
[10] M. de Dood, A. Polman, and J. Fleming, Phys. Rev. B **67**, 115106 (2003).
[11] S. David, M. El kurdi, P. Boucaud, A. Chelnokov, V. Le Thanh, D. Bouchier, and J. M. Lourtioz, Appl. Phys. Lett. **83**, 2509 (2003).
[12] A. Rogach, S. Kershaw, M. Burt, M. Harrison, A. Kornowski, A. Eychmüller, and H. Weller, Adv. Mater. (Weinheim, Ger.) **11**, 552 (1999).
[13] P. Olk, B. C. Buchler, V. Sandoghdar, N. Gaponik, A. Eychmller, and A. L. Rogach, Appl. Phys. Lett. **84**, 4732 (2004).
[14] M. Steinhart, J. H. Wendorff, A. Greiner, R. Wehrspohn, K. Nielsch, J. Schilling, J. Choi, and U. Gösele, Science **296**, 1997 (2002).
[15] N. Gaponik, D. Talapin, A. Rogach, A. Eychmüller, and H. Weller, Nano Lett. **2**, 803 (2002).
[16] H. Masuda and K. Fukuda, Science **268**, 1466 (1995).
[17] www.ab-initio.mit.edu/mpb